Tutor
Prof. Carlos M. Müller Jevenois
*Departament of Physical Chemistry*

Grau de Química

# Treball Final de Grau

**Galvanostatic electrodeposition and corrosion behaviour of gold-alloy coatings used in jewellery.**

Luis Alejandro Lanzetta López.

*June 2014.*

Universitat de Barcelona
Campus d'Excel·lència Internacional B:KC Barcelona Knowledge Campus

*Never lose a holy curiosity.*

Albert Einstein

I would like to show all my gratitude to Prof. Carlos M. Müller for teaching me so many things in such a short time. Without the knowledge I learned from him, it would have been impossible to write this report. I am also grateful for the time he spent giving me advice and supervising my work in an excellent and generous way.

I am also thankful to Víctor, who helped me countless times during lab work with his advice and experience in this field of chemistry. It was a pleasure to work side by side with him and share good conversations as well.

Very special thanks to Núria, who kindly agreed to help me with SEM and EDS measurements, even spending her own work time in lending a hand to me.

I would also like to thank Dr Ortega, Daniel, Albert and Edu for the help and the good moments I have spent with them these five months.

# REPORT

# CONTENTS

# 1. SUMMARY

Au-Cu-Cd alloys have been widely used in jewellery as decorative plating. Nowadays, Au-Cu-In alloys have progressively replaced the first mentioned one due to the high toxicity cadmium presents. In spite of this, there is no knowledge on Au-Cu-Cd in terms of corrosion behaviour, thus information to establish a comparative basis between both alloys is required. The aim of this study is to produce Au-Cu-Cd alloy coating samples by galvanostatic electrodeposition (a purchased alkaline cyanide bath was used for such a purpose) on metal substrates and evaluate their corrosion behaviour via electrochemical measurements. The influence of electrodeposition experimental parameters (current density, rotation speed of working electrode, substrate geometry) in terms of corrosion behaviour and alloy composition is reported as well. It was found out that low negative current densities induce the reduction of larger gold quantity on the substrate, therefore enhancing corrosion resistance. By its part, rotation speed does not seem to affect corrosion behaviour nor the alloy composition. The adaptation of large-scale conditions to lab-scale has been proved to have some limitations: while at industry area is not a determining parameter to obtain 75% Au alloys, only low substrate areas provide alloy coatings with such gold purity approximately under our laboratory conditions.

**Keywords**: Au-Cu-Cd alloy coatings, corrosion behaviour, galvanostatic electrodeposition, decorative plating, alkaline cyanide bath, polarization resistance, corrosion intensity.

# 2. RESUM

En el sector de la joieria, els aliatges de Au-Cu-Cd s'han fet servir àmpliament a mode de recobriments decoratius. No obstant, nous aliatges de Au-Cu-In han anat substituint progressivament els primers degut a l'alta toxicitat que el cadmi presenta. Malgrat tot, pràcticament no existeixen estudis sobre el comportament enfront la corrosió pel que fa a l'aliatge Au-Cu-Cd, requerint això que s'estableixi una base de comparació entre els dos. L'objectiu d'aquest estudi és produir mostres de recobriments de Au-Cu-Cd a través d'electrodeposició galvanostàtica (tot fent servir un bany alcalí cianurat) sobre substrats metàl·lics, així com avaluar el seu comportament enfront la corrosió mitjançant mesures electroquímiques. A més, s'esbrina la influència de diferents paràmetres experimentals de l'electrodeposició (densitat de corrent, velocitat de rotació de l'elèctrode de treball, geometria del substrat) en el comportament enfront la corrosió i la composició de l'aliatge. S'ha trobat que densitats de corrent negatives i baixes provoquen la reducció d'una major porció d'or a la composició de l'aliatge, augmentant així la resistència a la corrosió de la mostra. Per l'altra banda, la velocitat de rotació no sembla afectar el comportament enfront la corrosió ni la composició de l'aliatge. S'ha demostrat que l'adaptació al laboratori de les condicions de gran escala presenta algunes limitacions: mentre que, a la indústria, l'àrea no és un paràmetre determinant alhora d'obtenir aliatges amb un 75% d'or, només àrees petites de substrat sota les nostres condicions de laboratori proporcionen recobriments de tal puresa aproximadament

**Paraules clau**: recobriments d'aliatges de Au-Cu-Cd, comportament enfront la corrosió, electrodeposició galvanostàtica, recobriments decoratius, bany alcalí cianurat, resistència de polarització, intensitat de corrosió.

# 3. INTRODUCTION

As it is already known, electrochemical metal coatings comprehend a very wide range of features such as anti-adherence, abrasion-resistance, solid-film lubrication, chemical resistance, corrosion protection and decoration. Particularly, jewellery applications require both the two latter mentioned features. Normally, coatings used in jewels are made of noble metals (gold, platinum, rhodium, rhenium, silver, iridium, osmium, etc.) or alloys (using other support elements like copper, indium, etc.) that play the role of both preventing the substrate metal from corrosion (high standard reduction potential values of such elements; barrier between substrate and oxidizing medium) and giving the object a shiny and attractive aspect, as well as making the object acquire an added value.

## 3.1. AU-CU-CD TERNARY ALLOY

In jewellery sector, gold-copper-cadmium (Au-Cu-Cd) alloy coatings have been widely used as decorative plating. Evidently, the added value is given to the object by making gold the predominant metal in the alloy composition. For its part, copper enhances alloy coating hardness, since gold is a very soft metal by itself. Even in low quantities, cadmium improves the alloy coating behaviour towards corrosion, as well as making its mechanical properties considerably better.

However, industrial applications of cadmium are being progressively restricted due to the high toxicity (carcinogenic) such metal presents. The exposure of the human body to cadmium takes place mainly through inhalation and ingestion. Then, absorption through skin contact does not represent a serious risk for health. Nevertheless, the dangerousness of cadmium acquires importance when handled at industrial scale, with consequent problems in transport, storage, workers security and residue generation.

In order to replace cadmium in Au-Cu-Cd alloys, indium is currently being used in industry, providing the same properties to the ternary alloy (Au-Cu-In) that the first mentioned metal did and representing a non-toxic alternative.

Despite having been widely used in jewellery, there are practically no studies related to Au-Cu-Cd alloy in terms of corrosion behaviour. Although the use of cadmium has been suppressed, knowledge about such alloy is needed in order to establish a basis from which comparison with other ternary alloys (Au-Cu-In) can be done. Hence, this project focuses on the preparation of Au-Cu-Cd alloy coating samples through galvanostatic electrodeposition and the characterization of corrosion behaviour of such coatings by accelerating the process electrochemically.

## 3.2. ALKALINE CYANIDE BATH

Laboratory experiments performed for the purpose of this project were carried out imitating industrial conditions. For this, AuroloyTM 750 S (Enthone) was employed as electrochemical bath for electrodeposition, as well as it is made in large-scale conditions. The electrochemical bath is an aqueous alkaline solution of several components. The three metals that constitute the alloy are solved in the solution in the form of cyanide coordination complexes ($[Au(CN)_2]^-$, $[Cu(CN)_3]^{2-}$ and $[Cd(CN)_4]^{2-}$). Cyanide anions are present in excess in order to ensure the formation of the previously mentioned complexes and thus remaining a portion of free $CN^-$. Such complexes are the main ones for each metal, although it is possible to find other compounds with different coordination number due to cyanide association/dissociation processes1.

Apart from the metals, the electrochemical bath contains other substances or additives that help to obtain a coating with the desired properties. First of all, the levelling additives act by being adsorbed in high current density zones (peaks, surface defects), thus slowing alloy growth in such locations and levelling the surface of the electrodeposited layer, as depicted in Figure 1.

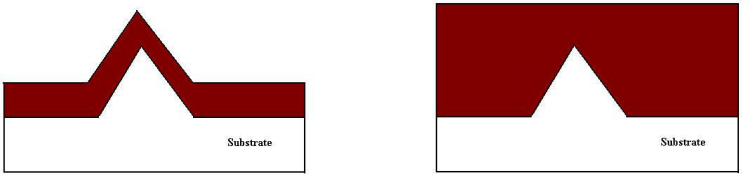


**Figure 1 –** Illustration of the action of leveling additives: electrodeposition with (right) and without additives (left).

The presence of levelling additives is crucial in embellishment terms, since a completely flat alloy surface provides shiny coatings.

Besides, structure modifiers perform the function of determining the preferential orientation and/or the crystalline structure of the alloy. His way, they act as internal stress diminishing agents.

Finally, wetting agents reduce surface tension at the solid-liquid interface, ensuring a good contact between both phases.

Despite knowing the criteria to classify the different types of additives, the composition of AuroloyTM 750 S is unknown due to industrial property protection.

Specifically, AuroloyTM 750 S is meant to be used to obtain a 18 carat (kt) alloy. Gold carat rating is an indication of the purity of a gold alloy. Its range goes from 0 to 24, meaning 0 that the alloy does not contain gold and 24 that there is actually no alloy due to a 100% purity gold. Then, 18 kt shows that the percentage of gold is 75%.

# 4. OBJECTIVES

The aim of this research work is the sample preparation of Au-Cu-Cd alloy coatings through galvanostatic electrodeposition and the electrochemical characterization of corrosion behaviour of coated samples doing measurements such as corrosion potential, polarization resistance, impedance and potentiodynamic polarization. Another purpose is to study the relationship between alloy composition and electrodeposition parameters (current density, rotation speed of the working electrode and system geometry), as well as making a comparison between two different substrate cleaning pre-treatments (electrolytic cathode degreasing and ultrasound treatment) in terms of coating surface homogeneity.

# 5. EXPERIMENTAL

## 5.1. SUBSTRATE PRE-TREATMENT AND GALVANOSTATIC ELECTRODEPOSITION OF AU-CU-CD ALLOY COATINGS

Samples of Au-Cu-Cd coatings were prepared via galvanostatic electrodeposition in a purchased alkaline cyanide bath (Auroloy™ 750 S, Enthone España S.A.). Before this, a cleaning pre-treatment was performed on each substrate in order to remove all the superficial organic matter. The electrodeposition was conducted at high temperature (68ºC) in a 500 mL glass cell using a standard three-electrode system.

### 5.1.1. Substrate preparation and cleaning pre-treatment

Several types of materials were used to make the substrates on which the gold-alloy coating was deposited. Such substrates consisted of flat metal sheets made of brass or iron (7 cm × 0,4 cm). The first ones were used either as obtained or with a 10 μm nickel coating. The effect of this layer is simple: it makes the substrate look shiny and its thickness is high enough to mask brass copper in future Energy-Dispersive X-ray Spectroscopy (EDS) elemental analysis of the Au-Cu-Cd alloy coating. Additionally, some substrates presented a thin palladium flash (0,1 μm) on the nickel layer in order to enhance the adherence of the ternary alloy.

The cleaning pre-treatment was done to eliminate all the organic matter from the surface of the substrates. Specifically, two different processes were performed for such a purpose: an electrolytic cathode degreasing and ultrasonic treatment. Concerning to the first mentioned one, two stainless steel plates constituted the anode, using each substrate as the cathode. The electrolyte of this system was a purchased aqueous alkaline solution that contained sodium hydroxide, sodium carbonate and other additives such as surfactants. Such surfactants play the role of easing the organic matter removal by diminishing surface tension at the solid-liquid interface to enhance its wetting. Through a galvanostatic process ($I \approx 0,1$ A), water reduction was induced in the cathode surface, thus appearing a hydrogen ($H_2$) bubbling around the substrate: these bubbles facilitate the detachment of the organic substances. The electrolytic medium was heated to 41-42ºC through a water bath prior to starting the cleaning process.

Once the electrolysis was performed, the substrates were submersed in distilled water to wash the excess of electrolyte and then placed inside a beaker with a purchased acidic solution with the purpose of neutralizing the alkali medium on the substrates surface and activating it towards electrodeposition (adherence enhancement). Again, the acidic solution contained surfactants that act the same way than the previously mentioned ones. Each substrate was then washed again with distilled water from a different beaker.

An alternative cleaning pre-treatment consisted of submersing the substrates in an ultrasounds bath using ethanol and water respectively. The exposure of samples to the acidic solution and consecutive water washing was also required to activate the surface.

### 5.1.2. Galvanostatic electrodeposition of Au-Cu-Cd alloy coating

A standard three-electrode cell (500 mL) was used in order to coat the substrates with the alloy. A cylindrical platinized titanium net was employed as the counter-electrode, while the metal sheets were used as the working electrode and the reference electrode was Ag/AgCl (NaCl 1 M) connected to a 16 g/L KCN Luggin capillary. The latter mentioned electrodes were located inside the cylinder with a specific purpose: in such arrangement, the distance between the working electrode and the counter-electrode is equal in all directions, thus contributing to a homogeneous alloy growth in both sides of the substrate (current intensities approximately equal in the entire surface). In order to ensure that such distance was invariable, it was required to carefully place the substrate in a perfect perpendicular arrangement with respect to the base of the cell. Moreover, electrodepositions were carried out under rotation of the working

electrode. The reason for this is that, when metals are reduced and electrodeposited on the substrate, the concentration of cyanide anions that constituted the complexes is increased significantly around the cathode (substrate) due to decomplexation. High cathodic $CN^-$ concentration causes the formation of more reactive Au cyanocomplexes, which can be electrodeposited on the substrate in an easier way. This means that the content of gold in the alloy would increase with detriment to the percentage of Cu (time-dependent concentrations), while Cd proportion stays invariable. Rotation of the substrate homogenizes $CN^-$ concentrations through mass-transport effects that seem to strongly affect alloy electrodeposition[2].

Table 1 shows the operation conditions of Auroloy™ 750 S bath and some properties of the eletrodeposited alloy, according to the specifications of its technical data sheet.

| | |
|---|---|
| **Au concentration (g/L)** | 4 (4-6) |
| **Cu concentration (g/L)** | 45 (45-60) |
| **Cd concentration (g/L)** | 1,0 (0,8-1,2) |
| **Free $CN^-$ concentration (g/L)** | 16 (16-20) |
| **pH** | 9,7 (9,5-10,0) |
| **Temperature (ºC)** | 67 (65-70) |
| **Cathodic efficiency (mg/A·min)** | 80 |
| **Substrate area ($dm^2$)** | 0,04 |
| **Coating thickness (µm)** | 3 |
| **Alloy density (mg/µm·$dm^2$)** | 145 |

**Table 1 –** Experimental specifications for Auroloy™ 750 S bath and properties of the Au-Cu-Cd electrodeposited alloy.

The next expression (1) provides the required charge in order to coat a substrate of a given area with a certain alloy thickness:

$$Q = d \cdot A \cdot \frac{\rho}{\eta} \quad (1)$$

**Q**: charge (A·min) **d**: thickness (µm) **A**: area ($dm^2$) **ρ**: alloy density (mg/µm· $dm^2$) **ŋ**: cathodic efficiency (mg/A·min)

Prior to alloy electrodepositing, it was required to settle the input current and the electrodeposition time. The charge values (A·min) equation 1 provides will enable the calculation of the electrodeposition time in minutes as a second setting.

16 samples were prepared following the parameters (type of substrate, current density, electrodeposition time and rotation speed) shown in Table 2:

| Sample | Type of substrate | Area ($cm^2$) | Time (min) | Rotation speed (rpm) | Applied current (A) | Current density (A/dm) |
|---|---|---|---|---|---|---|
| GAL1 | Brass/Ni/Pd flash | 4,72 | 6 | 20 | -0,04 | -0,85 |
| GAL 2 | Brass/Ni/Pd flash | 4,84 | 6 | 20 | -0,04 | -0,83 |
| GAL 3 | Brass/Ni/Pd flash | 4,89 | 6 | 20 | -0,04 | -0,82 |
| GAL 4 | Brass/Ni/Pd flash | 5,17 | 6 | 20 | -0,04 | -0,77 |
| GAL 5 | Brass/Ni/Pd flash | 4,77 | 11 | 20 | -0,02 | -0,42 |
| GAL 6 | Brass/Ni/Pd flash | 5,17 | 4 | 20 | -0,06 | -1,16 |
| GAL 7 | Brass/Ni/Pd flash | 5,03 | 11 | 20 | -0,02 | -0,39 |
| GAL 8 | Brass/Ni/Pd flash | 5,79 | 6 | 30 | -0,04 | -0,69 |
| GAL 9 | Brass/Ni/Pd flash | 5,62 | 6 | 25 | -0,04 | -0,71 |
| GAL 10 | Brass | 5,55 | 6 | 20 | -0,04 | -0,72 |
| GAL 11 | Brass/Ni | 4,74 | 6 | 20 | -0,04 | -0,84 |
| GAL 12 | Iron | | 6 | 20 | -0,04 | |
| GAL 13 | Brass/Ni | 5,46 | 6 | 20 | -0,04 | -0,73 |
| GAL 14 | Brass/Ni | 5,50 | 6 | 0 | -0,04 | -0,73 |
| GAL 15 | Brass/Ni/Pd flash | 4,51 | 6 | 20 | -0,04 | -0,89 |

| | | | | | | |
|---|---|---|---|---|---|---|
| GAL 16 | Brass/Ni/Pd flash | 4,15 | 6 | 20 | -0,04 | -0,96 |
| GAL 18 | Brass/Ni/Pd flash | 4,00 | 6 | 20 | -0,04 | -1,00 |
| GAL 19 | Brass/Ni/Pd flash | 4,00 | 6 | 20 | -0,04 | -1,00 |
| GAL 20 | Brass/Ni/Pd flash | 4,00 | 6 | 20 | -0,04 | -1,00 |
| GAL 21 | Brass/Ni/Pd flash | 4,00 | 6 | 20 | -0,04 | -1,00 |
| GAL 25 | Brass/Ni/Pd flash | 0,50 | 6 | 20 | -0,005 | -1,00 |
| GAL 26 | Brass/Ni/Pd flash | 4,00 | 6 | 40 | -0,04 | -1,00 |
| GAL 27 | Brass/Ni/Pd flash | 2,00 | 6 | 20 | -0,02 | -1,00 |
| GAL 28 | Brass/Ni/Pd flash | 1,00 | 6 | 20 | -0,01 | -1,00 |

**Table 2 –** Samples prepared via galvanostatic electrodeposition and followed parameters. All substrates were pre-treated by electrolytic cathode degreasing except for GAL 16-GAL 28 (ultrasonic treatment).

As it can be observed in Table 2, area must be measured in each case in order to determine current density. Time values were obtained through charge values provided by equation 1. However, times selected as input settings were an approximation to the closest higher integer number.

Three different Auroloy™ 750 S baths were used to prepare the samples. GAL1-GAL14 were obtained using Bath 1. Hence, GAL 15 and GAL 16 were created using Bath 2, while GAL 18-GAL 28 were prepared from Bath 3. All three baths were chemically equal except for Bath 2, which was modified by adding an aliquote of nitriloacetic acid solution (NTA, concentration: 500 g/L).

Once electrodeposition was performed, all samples were rinsed with distilled water and kept covered with laboratory tissue until measuring their corrosion behavior in order to avoid contamination.

## 5.2. CORROSION MEASUREMENTS OF AU-CU-CD ALLOY SAMPLES

All corrosion measurements were taken using a three-electrode electrochemical system, where the samples were used as the working electrode (Figure 2).

**Figure 2 –** Experimental setup for corrosion measurements (left: counter-electrode; middle: sample; right: reference electrode).

The reference electrode was Ag/AgCl (NaCl 1 M) connected to a NaCl 5% Luggin capillary and the counter-electrode was a platinized titanium net. The electrolyte used in such measurements had to be chosen carefully: it was required to reproduce an aggressive enough medium to test the samples under as realistic as possible conditions (e.g. sweat). For such a purpose, a rock salt solution (5% w/w) was chosen (200 mL). $Cl^-$ anions are well-known for their depassivating properties: they have the same charge and are quite similar to $OH^-$ anions (located in hydrated oxide layers) in terms of size so they can replace them, thus making passivating layers soluble. In order to minimize environmental noise, the whole experimental setup was placed inside a Faraday cage (Figure 3).

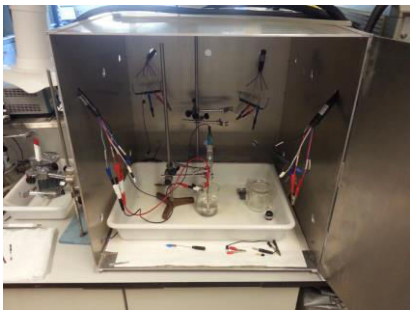

**Figure 3 –** Faraday cage used to keep the experimental setup safe from noise.

The surface of each sample exposed to the saline solution was 2 $cm^2$. In order to reduce the contact area of the samples, varnish was used to mask a part of the alloy.

### 5.2.1. Corrosion potential test

The first measurement that was performed in all samples was corrosion potential test, which basically consists of monitoring open circuit voltage ($E_{oc}$, a.k.a. $E_{corr}$) depending on time (no current is being applied). The aim of this test is the characterization of the alloy coating: samples are not equal to each other, so the processes that take place in the metallic surface-solution interface occur with a different importance or even different processes happen in each case. This variability is translated as a different value for corrosion potential ($E_{corr}$) for each single sample. The data recording ends once voltage remains constant or after a previously established time.

### 5.2.2. Polarization resistance

Polarization resistance experiments were carried out by recording current versus voltage as the cell voltage was swept over a small range of potential close to $E_{oc}$ ($E_{oc}$ ± 5 mV), thus obtaining a straight line. A numerical fit of the line provides a value for the slope, which is the polarization resistance ($R_p$). This resistance shows the opposition to the flow of current caused by an electrochemical reaction (corrosion process) at the solid-liquid interface. Hence, large values of $R_p$ denote a better performance of a metal towards corrosion. The term “polarization” is used due to the input signal that is applied to the sample, that forces away potential from its value at $E_{corr}$.

### 5.2.3. Impedance

Impedance experiments consisted of applying an oscillating input potential and recording an oscillating output current. Through Ohm’s Law, it is possible to obtain a value of impedance depending on frequency (20000 kHz – 1000 mHz). Impedance has two contributions at such frequency range: resistance (Z’) and reactance (capacitative elements, Z’’). They both are represented in a complex plane, being resistance the real coordinate and reactance the imaginary coordinate. The result of an impedance experiment is a representation of resistance versus negative reactance (Nyquist impedance plot). This plot presents a semi-circular shape at high-frequency/low-resistance values that turns into linear in low-frequency/high-resistance

regions. Semi-circular shape is related to charge-transfer control of the electrochemical process, while linear behaviour is connected to mass-transfer phenomena[3] (Figure 4).

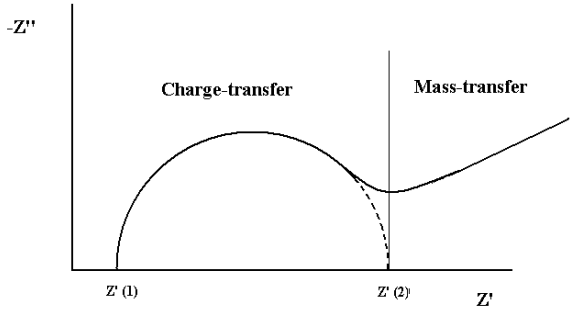


**Figure 4 –** Nyquist impedance plot. Notice that two different regions can be distinguished (mass-transfer control: high resistance; charge-transfer control: low resistance)

Thus, impedance techniques are useful to characterize and differentiate the processes that are taking place in an interface depending on frequency, as well as to determine $R_p$ by subtracting Z' (1) to Z'(2).

### 5.2.4. Potentiodynamic polarization

Potentiodynamic polarization (PP) is a voltamperometric technique that involves the application of a linear potential sweep to working electrode while current is registered. For all samples, potential sweep was performed increasing the value of applied voltage with time, showing an initial reduction process followed by an oxidation. Logarithm of total current depending on applied potential was represented as the result of the experiment. It is worth minding that current is the result of summing current values of cathodic (negative total current values, reduction of the oxidizing agent in the medium) and anodic (positive total current values, oxidation of the metal) processes. In charge transfer control regions, classic Tafel analysis was performed by extrapolating the linear portions of a log (I) vs. potential plot back to their intersection, making it coincide with the corrosion potential. When $E=E_{corr}$, value of total current is zero. The reason for this is that anodic and cathodic current achieve the same absolute value

with inverted signs, so they annul each other. Such absolute value coincides with corrosion current ($I_{corr}$) at the previously mentioned intersection upon $E_{corr}$ (Figure 5).

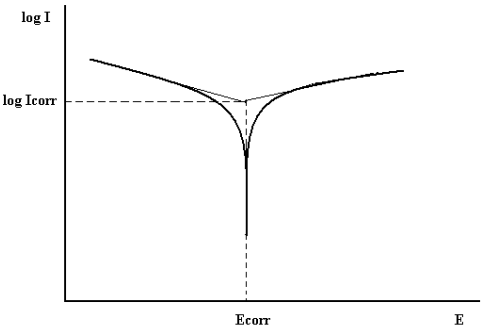


**Figure 5 –** PP plot with a demonstration of classic Tafel analysis.

$I_{corr}$ is a kinetic parameter that is directly proportional to the corrosion rate of the metal. Hence, high $I_{corr}$ values show great tendency of the metal to corrode in a certain medium and vice-versa.

## 5.3. SAMPLE ELEMENTAL ANALYSIS AND IMAGE ACQUISITION

The aim of elemental analysis of the Au-Cu-Cd alloy was to check if any of the studied variables when electrodepositing (current density, rotation speed and system geometry) affected the proportion of each metal in the deposit and thus the corrosion behaviour of the sample. Also, morphology information was required to test which of the degreasing methods was preferable in terms of surface homogeneity: it was suspected that $H_2$ generated during electrolytic cathodic degreasing could be absorbed by the Pd flash outer layer, since such metal presents exceptional hydrogen-absorbing properties. The absorbed gas was likely to be released at high temperature (68ºC) during the electrodeposition, with the inconvenience of irregular alloy electrodeposition (bubble formation, defects, etc.).

Two microscopy techniques were used: Scanning Electron Microscopy (SEM) and Optical Microscopy (OM). Images of substrate morphology were obtained via both microscopes, while the elemental analysis of samples was performed through EDS.

# 6. RESULTS AND DISCUSSION

## 6.1. CORROSION CHARACTERIZATION

Most of the samples listed in Table 2 were tested in corrosion measurements. The results of the corrosion behaviour each sample presented are shown in Table 3.

| Sample | Ecorr (V) | Rp(ohm) | Rp via AC (Ω) | Icorr (µA) | Ecorr via PP (V) | βc (mV) | βa (mV) | Icorr via SG (µA) |
|---|---|---|---|---|---|---|---|---|
| GAL 1 | -0,11 | 22391 | 23653 | 0,82 | -0,1 | 53,4 | 81,5 | 0,63 |
| GAL 2 | -0,11 | 17706 | 14404 | 0,76 | -0,111 | 61 | 89,3 | 0,89 |
| GAL 3 | -0,107 | 4443 | 4080 | 3,40 | -0,135 | 94,6 | 121,5 | 5,20 |
| GAL 4 | -0,103 | 8663 | 9459 | 2,23 | -0,11 | 96 | 123,61 | 2,71 |
| GAL 5 | 0 | 149634 | 183434 | 0,07 | -0,006 | 61,4 | 91,7 | 0,11 |
| GAL 6 | -0,031 | 5725 | 5573 | 1,99 | -0,074 | 85,4 | 78,5 | 3,11 |
| GAL 7 | -0,101 | 28000 | 28118 | 0,57 | -0,135 | 73,5 | 115,5 | 0,70 |
| GAL 8 | -0,159 | 7562 | 7099 | 2,49 | -0,156 | 111,8 | 84,9 | 2,77 |
| GAL 9 | -0,102 | 16933 | 19733 | 0,72 | -0,112 | 85,9 | 98,6 | 1,18 |
| GAL 10 | -0,117 | 7329 | 9625 | 1,64 | -0,134 | 101,9 | 105,1 | 3,07 |
| GAL 11 | -0,118 | 8929 | 10344 | 1,98 | -0,119 | 102,4 | 129,6 | 2,79 |
| GAL 18 | -0,142 | 12301 | 12755 | 1,16 | -0,146 | 85,8 | 118,1 | 1,76 |
| GAL 19 | -0,073 | 54898 | 56285 | 0,22 | -0,116 | 43,8 | 79,5 | 0,22 |
| GAL 20 | -0,15 | 15218 | 15779 | 1,12 | -0,161 | 82,4 | 115,4 | 1,37 |
| GAL 21 | -0,143 | 20000 | 20898 | 0,95 | -0,144 | 90,7 | 125,9 | 1,15 |

**Table 3 -** Results of corrosion measurements for samples GAL 1-GAL 11 and GAL 18-GAL 21.

Since $I_{corr}$ cannot be measured directly, $I_{corr}$ via SG (Stern-Geary Equation, 2) was calculated in order to verify that the method used to obtain $I_{corr}$ (classic Tafel analysis) is valid and was done properly (values in both columns coincide in their order of magnitude, proving reliable Tafel data analysis).

$$Icorr = \frac{\beta a \cdot \beta c}{2{,}303 \cdot (\beta a + \beta c) \cdot Rp} \quad (2)$$

Similarly, $R_p$ values obtained via polarization resistance and impedance tests do not differ much from each other. Thus, there is no difference in choosing ones or others when making comparisons between samples. In the previously shown table, there are also two columns referring to $E_{corr}$. The difference between them is that PP values were obtained once all other

corrosion measurements were performed in comparison with the other values (obtained firstly). As it can be observed, there are evident differences between both groups of values, being those obtained via PP more negative ($E_{corr}$ evolves during the corrosion experiment). This is a clear evidence that corrosion measurements made on the samples before performing PP affect the value of $E_{corr}$, being this an indication of a variation in the interface system.

As the results in Table 3 show, samples do not seem to be fully reproducible in terms of corrosion behaviour. This means that samples made under the same conditions exhibit different values of $I_{corr}$ and $R_p$. For instance, GAL 1, GAL 2 and GAL 3 were prepared with equal rotation speeds and at very similar current densities (-0,85 A/dm$^2$, -0,83 A/dm$^2$ and -0,82 A/dm$^2$, respectively, as shown in Table 2), but they show different results after corrosion measurements (Figures 6, 7 and 8):

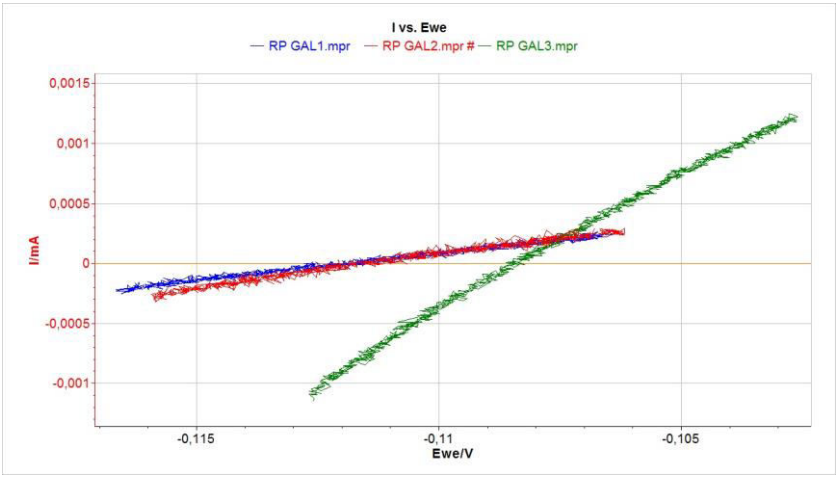


**Figure 6 –** $R_p$ plots of samples GAL 1, GAL 2 and GAL 3.

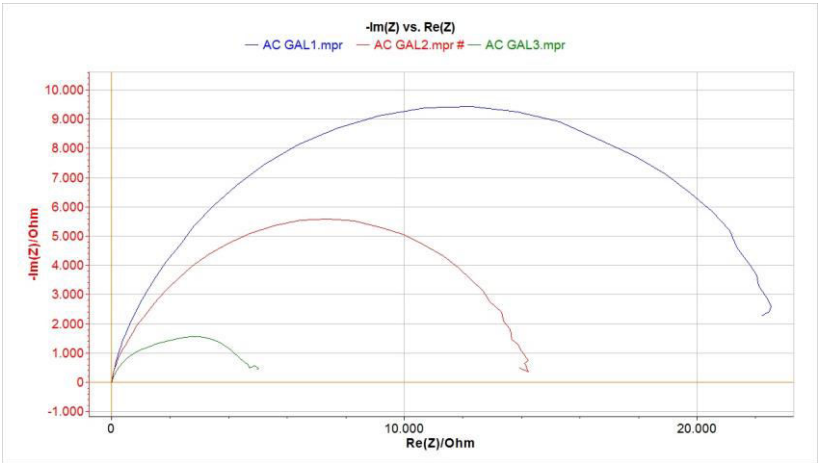


**Figure 7 –** Impedance plots of samples GAL 1, GAL 2 and GAL 3. Re is for "real axis" and Im for "Imaginary axis".

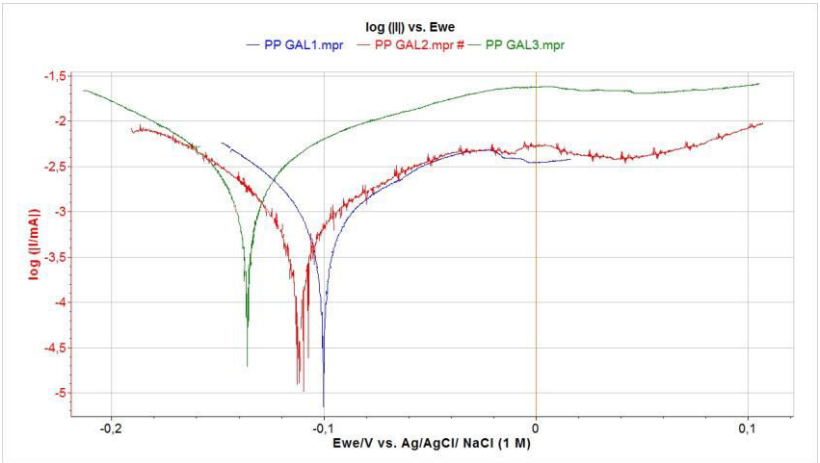


**Figure 8 –** PP plots of samples GAL1, GAL2 and GAL3. Pulses in GAL2 appear due to noise.

There are significant differences in $R_p$ values according to data shown in Figures 6, 7 and 8. In Figure 6, the slope for GAL 3 is significantly higher in comparison to GAL 1 and GAL 2. As

explained above, this means that $R_p$ is considerably lower (Ohm's Law: I = V/R, the slope of the I vs. E representation corresponds to 1/R) for the first mentioned sample, thing that can also be pointed out in Figure 7. The differences between GAL 1 and GAL 2 are also noticeable. In terms of $I_{corr}$, there is a clear difference between samples: while values for GAL 1 and GAL 2 remain similar, GAL 3 data provides higher $I_{corr}$ values (its PP plot is shifted upwards).

Low values of $R_p$ and high values of $I_{corr}$ show a higher tendency of samples to experiment interface red-ox processes, thus having a poorer resistance towards corrosion. According to the previously shown data, corrosion behaviour is better in the following order: GAL 1, GAL 2 and GAL 3.

In order to find an explanation to such differences in corrosion behaviour even in equally prepared samples, EDS elemental analysis was performed (Table 4):

| Sample | Gold (%) | Copper (%) | Cadmium (%) |
|---|---|---|---|
| GAL 1 | 54,24 | 39,04 | 6,72 |
| GAL 2 | 50,53 | 41,87 | 7,59 |
| GAL 3 | 50,80 | 43,40 | 5,80 |

**Table 4 –** EDS microanalysis elemental weight proportion of samples GAL 1, GAL 2 and GAL 3.

It is clear that samples considered above do not show big differences between them in terms of composition. Then, the worse corrosion behaviour of GAL 3 might be caused by the smaller percentage of cadmium that the alloy presents (it must be remembered that cadmium provides better corrosion behaviour even in small quantities).

Another fact that can justify the different corrosion behaviour in such three samples is the acquired stationary potential while galvanostatic electrodeposition was being performed, as shown in Figure 9.

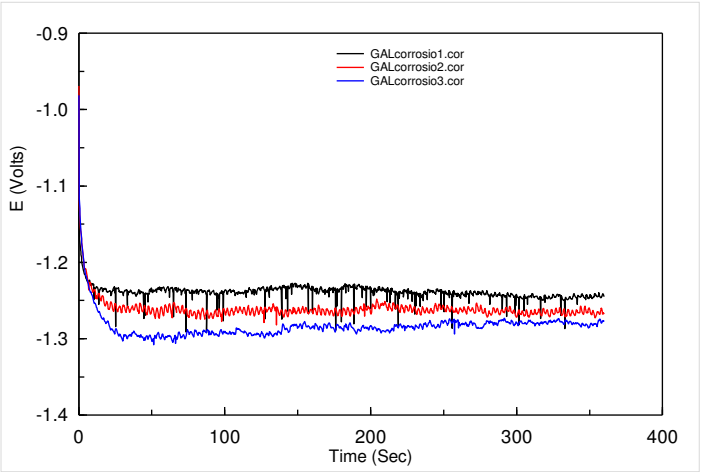


**Figure 9 –** Time evolution of potential during galvanostatic electrodeposition of samples GAL 1, GAL 2 and GAL 3. Peaks in GAL 1 correspond to noise.

As depicted above, stationary potential grows negatively from GAL 1 to GAL3, just as the worsening observed in their corrosion behaviour. Differences in stationary potential while electrodeposition is taking place can induce the formation of different alloy crystalline structures without altering the coating elemental composition. Such different atomic arrangements might not behave the same way towards corrosion.

The lack of reproducibility towards corrosion behaviour is not only related to composition, but also to the particular casuistry of each substrate (surface defects, scratches, bending, etc.). This might be an explanation to the observed differences between stationary potentials in Figure 9. In addition, dispersion in $E_{corr}$ values between samples might also be related to differences in corrosion behaviour.

The difficulty to obtain samples with invariable corrosion behaviour has been justified and

discussed. However, the electrochemical window in terms of composition does not seem to be so small: GAL 1, GAL 2 and GAL 3 were prepared at current densities of -0,85 A/dm$^2$, -0,83 A/dm$^2$ and -0,82 A/dm$^2$ while GAL 18 and GAL 19 were obtained at -1,00 A/dm$^2$ (composition data shown in Table 5). In both groups of samples, gold percentage in the alloy coating is very similar (around 52-53% approximately or 12 kt).

| Sample | Gold (%) | Copper (%) | Cadmium (%) |
|---|---|---|---|
| GAL 18 | 54,41 | 40,08 | 5,51 |
| GAL 19 | 53,45 | 40,72 | 5,82 |

**Table 5 -** EDS microanalysis elemental weight proportion of samples GAL 18 and GAL 19.

## 6.2. CORROSION BEHAVIOUR VS. CURRENT DENSITY

Obviously, the electrochemical window mentioned above has some limitations. There are clear differences in corrosion behaviour between samples prepared at very different current densities. For instance, samples GAL 1, GAL 5, GAL 6 and GAL 7 (-0,85 A/dm$^2$, -0,42 A/dm$^2$, -1,16 A/dm$^2$ and -0,39 A/dm$^2$, respectively) exhibited different behaviour towards corrosion (Figures 10 and 11).

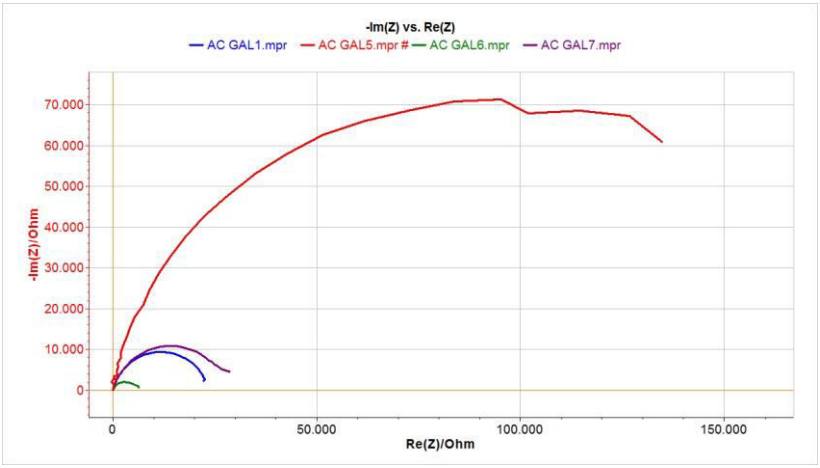


**Figure 10 –** Impedance plots of samples GAL 1, GAL 5, GAL 6 and GAL 7.

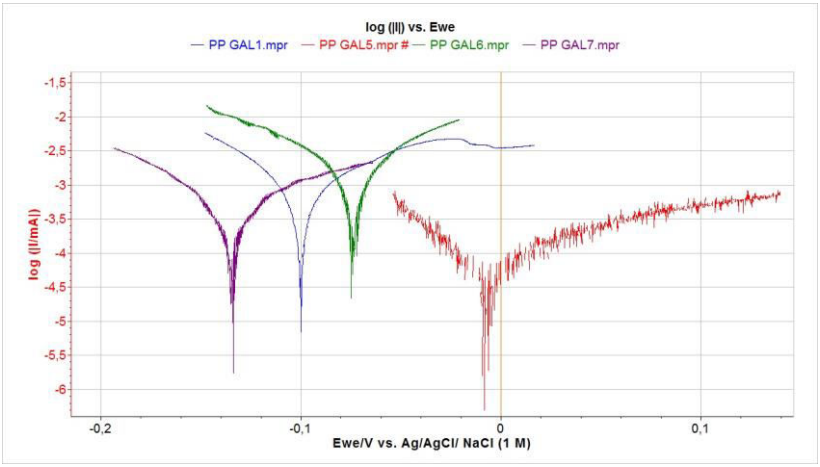


**Figure 11 –** PP plots of samples GAL 1, GAL 5, GAL 6 and GAL 7.
Inaccuracies in GAL5 are related to noise problems.

For its part, GAL 6 presented the lowest resistance to corrosion among the group ($R_p$ = 5600 Ω, $I_{corr}$ = 2 μA), showing the smallest semicircle in impedance measurements. GAL 1 corrosion behaviour was better than the previous sample ($R_p$ = 23000 Ω, $I_{corr}$ = 0,82 μA), but not superior to GAL 5 ($R_p$ = 165000 Ω, $I_{corr}$ = 0,07 μA) and GAL 7 ($R_p$ = 28000 Ω, $I_{corr}$ = 0,57 μA), as depicted.

It seems clear that corrosion behaviour is improved when current density decreases, as demonstrated above. Once again, a better resistance to corrosion can be related to composition via EDS microanalysis (Table 6).

| Sample | Gold (%) | Copper (%) | Cadmium (%) |
|---|---|---|---|
| GAL 1 | 54,24 | 39,04 | 6,72 |
| GAL 5 | 71,40 | 24,9 | 3,70 |
| GAL 6 | 31,71 | 55,95 | 3,67 |
| GAL 7 | 73,75 | 19,54 | 6,72 |

**Table 6 -** EDS microanalysis elemental weight proportion of samples GAL 1, GAL 5, GAL 6 and GAL 7.

According to the composition results, an increase in electrodeposition current density makes composition poorer in gold and richer in copper. This is the reason why low current density samples exhibit better corrosion behaviour than those prepared at high current densities (higher proportion of a noble metal).

Differences between GAL 5 and GAL 7 in terms of corrosion behaviour are evident, despite having been prepared at similar current densities. However, their respective compositions do not differ much from each other, as shown in Table 6. One more time, this differential behaviour is related to the particular casuistry of each sample, especially in the case of GAL 5 (much difference when compared to the others). As it was mentioned above, substrate particularities can be linked to different $E_{corr}$ values, being them characteristic of each single case.

In the case of this particular comparison, it was possible to show corrosion behaviour visually. Noticeably, GAL 6 was the sample which showed less corrosion resistance and even pitting was visible on its surface. SEM images of samples GAL 6 and GAL 7 show the effect of corrosion tests on both surfaces (Figure 12):

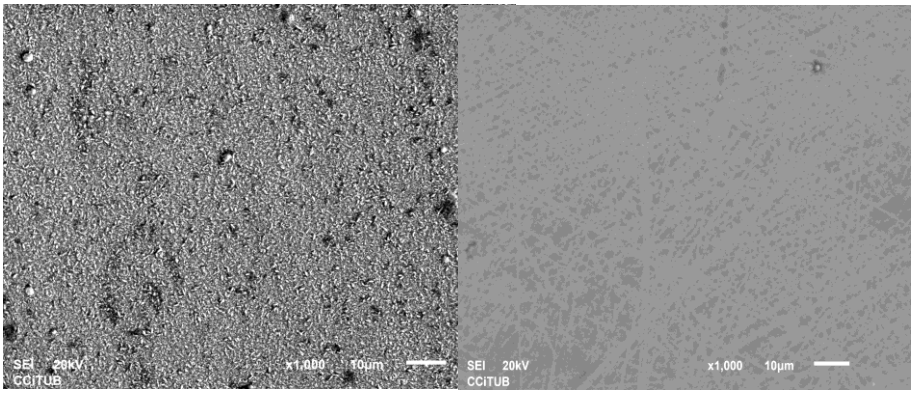


**Figure 12 –** SEM images (x1000) of samples GAL6 (left) and GAL7 (right). Grains observed in GAL6 are problably oxide microcrystals, while GAL7 exhibits a clean surface with only some small scratches caused by prolonged storage.

## 6.3. CORROSION BEHAVIOUR VS. ROTATION SPEED

Samples GAL 8, GAL 9 and GAL 10 were prepared at very similar current densities (-0,69 A/dm$^2$, -0,71 A/dm$^2$ and -0,72 A/dm$^2$, respectively). The factor that was varied during electrodeposition was rotation speed (30 rpm, 25 rpm and 20 rpm). As shown in Table 3, corrosion behaviour does not follow a linear trend when changing rotation speed. GAL 9 presented better corrosion behaviour (Rp = 18500 Ω, Icorr = 0,72 µA) than GAL 8 (Rp = 7250 Ω, Icorr = 2,49 µA) and GAL 10 (Rp = 8450 Ω, Icorr = 1,64 µA). This seems to show that the optimal rotation speed is around 25 rpm in terms of corrosion resistance.

Concerning composition, there is not a big difference between GAL 8 and GAL 9, as shown in Table 7, while GAL 14 (prepared without rotation) has a lack of gold:

| Sample | Gold (%) | Copper (%) | Cadmium (%) |
|---|---|---|---|
| GAL 8 | 47,40 | 44,80 | 7,80 |
| GAL 9 | 51,70 | 41,50 | 6,80 |
| GAL 14 | 41,70 | 53,40 | 4,90 |

**Table 7 -** EDS microanalysis elemental weight proportion of samples GAL 8 and GAL 9.

Composition data in Table 7 and the fact that GAL 14 was affected more evidently by rotation speed in such terms demonstrate that the electrodeposition process is regulated by mass-transfer control[2].

## 6.4. COMPOSITION VS. SYSTEM GEOMETRY

Apart from current density and rotation speed influence on corrosion behaviour, substrate geometry and its effect on composition were also studied. EDS microanalysis was performed in order to find out composition in samples GAL 25, GAL 26, GAL 27 and GAL 28 (Table 8). System geometry was varied by changing the area of each substrate (0,5 cm$^2$, 4 cm$^2$, 2 cm$^2$ and 1 cm$^2$). It must be noticed that GAL 26 was prepared with 40 rpm rotation and not at 20 rpm as the rest of considered samples. This fact should not be taken into consideration when

comparing the effect of substrate area, since the influence of rotation speed is relatively low as mentioned above. Current density was -1 A/dm$^2$ for all samples.

| Sample | Gold (%) | Copper (%) | Cadmium (%) |
|---|---|---|---|
| GAL 25 | 71,50 | 20,20 | 8,30 |
| GAL 26 | 53,49 | 39,42 | 7,09 |
| GAL 27 | 54,66 | 39,84 | 5,49 |
| GAL 28 | 60,66 | 33,59 | 5,75 |

**Table 8 -** EDS microanalysis elemental weight proportion of samples GAL 25, GAL 26, GAL 27 and GAL 28.

As showed above, increase of gold percentage in the alloy is observed when substrate area becomes smaller. In fact, gold portion in GAL 25 (71,50%) is quite close to expected 75% that this electrochemical bath should provide (18 kt).

## 6.5. CLEANING PRE-TREATMENTS COMPARISON

Samples GAL 15 and GAL 16 were specifically prepared in order to compare the effect of two different cleaning pre-treatments: cathodic degreasing and ultrasounds bath. The initial hypothesis that encouraged this comparison was that the Pd flash layer of the substrates was likely to absorb hydrogen generated during cathodic degreasing, and such hydrogen could be released afterward during the electrodeposition at 68ºC, thus forming bubbles and not smooth coating surface. OM images (Figure 13) were taken to explore the surface of both samples at micron scale to see if cathodic degreasing sample (GAL 15) presented more imperfections than ultrasounds bath sample (GAL 16).

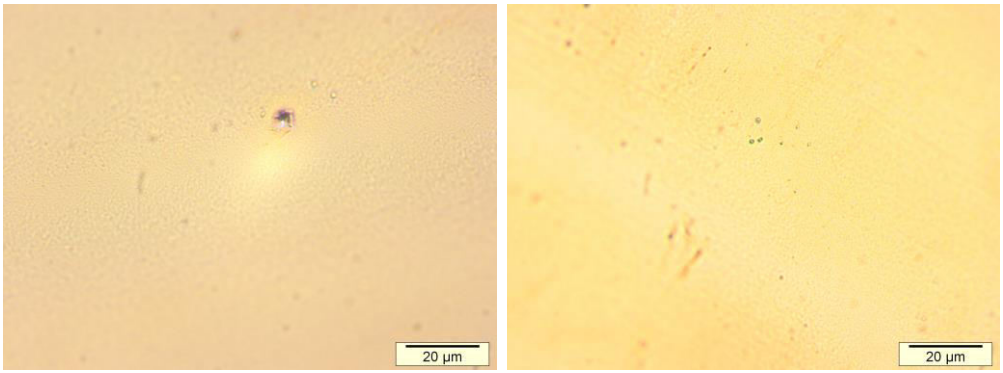


**Figure 13 –** OM images of samples GAL 15 (left) and GAL 16 (right).

As depicted, there are no clear differences between both images at micron scale. Then, the hydrogen-absorbing effect of Pd does not seem to affect the alloy coating regularity. Probably, higher thickness of Pd (Pd flash thickness: 0,1 µm) would present more problems in this way. Another argument on this point is that the time the substrate remains submersed in the electrochemical bath at 68ºC prior to electrodeposition may be enough to release the majority of the absorbed hydrogen. It is true that the image corresponding to GAL15 shows an imperfection, but does not seem to have been made by a hydrogen bubble. In fact, it is likely that such feature in GAL15 surface is an alloy agglomerate.

# 7. CONCLUSIONS

It has been shown that differences in corrosion behaviour among samples made under the same conditions are related to compositional variations. Specifically, cadmium composition plays a vital role at defining the corrosion response of the ternary alloy coating: a lack of such metal in a sample makes the decorative plating more prone to experiment corrosion compared to another sample with higher cadmium amount in its composition, even considering similar gold proportion in both. Moreover, differences in corrosion behaviour of equally made samples can also be justified by analysing the values of stationary potential that samples acquired during

electrodeposition: high negative values of E are related to less corrosion resistance. Such fact seems to find an explanation if it is taken into consideration that variation in stationary potential induces the electrodeposition of different crystalline phases of the alloy (different tendency to corrosion depending on the structure). Finally, it must also be considered that each substrate has its own particularities (e.g. defects), so casuistry plays a very important role in corrosion behaviour. This factor may even be related to variability in stationary potential and $E_{corr}$.

Evidences on the dependence of corrosion behaviour in electrodeposition current density have been provided: corrosion behaviour tends to be worse (less corrosion resistance) as current density is increased. Thus, such fact is related to alloy composition, which becomes richer in gold and poorer in copper when current density decreases (samples richer in gold experiment enhanced corrosion behaviour due to the noble nature of such metal).

Concerning rotation speed, samples prepared at 25 rpm under the same current density conditions showed better response towards corrosion, without noticeable differences in composition. A dramatic drop of gold content in samples prepared without rotation demonstrates that the electrodeposition is controlled by mass-transfer processes.

The effect of system geometry has a huge importance in alloy composition. It has been shown that electrodeposition performed on substrates with smaller areas provides samples richer in gold, even under the same current density and rotation conditions. Experimental work shows that the optimal substrate area is around 0,5 $cm^2$ if ~18 kt alloy is wanted. In jewellery industry, area is not a limiting parameter and this demonstrates the existence of limitations when reproducing industrial conditions at small scale. Such limitations may be related to different hydrodynamic conditions (rotation) in comparison to industry.

Both cleaning pre-treatments were compared and discussed: there is no evidence proving that cathodic degreasing is worse in terms of alloy surface homogeneity (the effect of absorbed hydrogen in the Pd flash layer is not observed).

# 8. REFERENCES

1. Brun, E.; Durut, F.; Botrel, R.; Theobald, M.; Legaie, O.; Popa, I.; Vignal, V. Influence of the Electrochemical Parameters on the Properties of Electroplated Au-Cu Alloys. *J. Electrohem. Soc.* **2011**, *158(4),* D223-D227.
2. Bozzini, B.; Cavallotti, P.L. Electrodeposition and Characterization of Au-Cu-Cd Alloys B. *J. Appl. Electrochem.* **2001,** *31*, 897-903.
3. Brett, C.M.A.; Brett, A.M.O. Electrochemistry: principles, methods and applications. Oxford: Oxford University Press, **1993**.

# 9. ACRONYMS

**EDS**: Energy-Dispersive X-Ray Spectroscopy.

**NTA**: nitriloacetic acid.

**PP**: Potentiodynamic Polarization.

**SEM**: Scanning Electron Microscopy.

**OM**: Optical Microscopy.

**SG**: Stern-Geary Equation.